Langenbeck's Archives of Surgery (2021) 406:251–259
https://doi.org/10.1007/s00423-020-01966-0

REVIEW ARTICLE

Quantification of fluorescence angiography: Toward a reliable intraoperative assessment of tissue perfusion - A narrative review

Christian Dam Lütken[1,2] · Michael P. Achiam[1] · Jens Osterkamp[1] · Morten B. Svendsen[3] · Nikolaj Nerup[1]

Received: 6 August 2020 / Accepted: 9 August 2020 / Published online: 21 August 2020
© Springer-Verlag GmbH Germany, part of Springer Nature 2020

Abstract

Background Accurate intraoperative assessments of tissue perfusion are essential in all forms of surgery. As traditional methods of perfusion assessments are not available during minimally invasive surgery, novel methods are required. Here, fluorescence angiography with indocyanine green has shown promising results. However, to secure objective and reproducible assessments, quantification of the fluorescent signal is essential (Q-ICG). This narrative review aims to provide an overview of the current status and applicability of Q-ICG for intraoperative perfusion assessment.

Results Both commercial and custom Q-ICG software solutions are available for intraoperative use; however, most studies on Q-ICG have performed post-operative analyses. Q-ICG can be divided into inflow parameters (*ttp*, *t*0, slope, and $T_{1/2}$max) and intensity parameters (*F*max, PI, and DR). The intensity parameters appear unreliable in clinical settings. In comparison, inflow parameters, mainly slope, and $T_{1/2}$max have had superior clinical performance.

Conclusion Intraoperative Q-ICG is clinically available; however, only feasibility studies have been performed, rendering an excellent usability score. Q-ICG in a post-operative setting could detect changes in perfusion following a range of interventions and reflect clinical endpoints, but only if based on inflow parameters. Thus, future studies should include the methodology outlined in this review, emphasizing the use of inflow parameters (slope or $T_{1/2}$max), a mass-adjusted ICG dosing, and a fixed camera position.

Keywords Quantitative fluorescence angiography · Optimization · Indocyanine green · Intraoperative · Perfusion assessment

Background

Visceral tissue viability is mainly dependent on adequate tissue perfusion [1–3], and compromised tissue perfusion during surgery is a significant risk factor for complications such as anastomotic leakage (AL) [4–7]. AL is a severe surgical complication associated with significantly increased health expenses, increased length of hospitalization, increased risk of recurrence after oncological resection, and reduced survival [8–11]. Thus, securing adequate perfusion during gastrointestinal surgery is essential. Perfusion assessment has historically been performed based on visual and tactile cues such as tissue color, peristalsis, bleeding at the resection line, and palpation of the mesenteric pulse [12]; however, perfusion assessment by surgeons have shown low sensitivity and specificity for AL [13]. Also, these methods are subjective in nature and not applicable during laparoscopic surgery [13], when combined with an increasing number of robotic and laparoscopic procedures, a new method for perfusion assessment is required [14, 15].

A promising method for perfusion assessment is fluorescence angiography (FA) with indocyanine green (ICG). ICG is a tricarbocyanine dye with extremely few adverse events; it binds to lipoproteins in plasma, has a short plasma half-life (2–4 min), is metabolized exclusively in the liver, and is excreted unmodified in the bile [16, 17]. The microvascular flow, i.e., perfusion, is considered proportional to the fluorescence signal, generated by illuminating the tissue with near-infrared light, during the first-time ICG passage [18].

✉ Christian Dam Lütken
Christianlutken@gmail.com

[1] Department of Surgical Gastroenterology, Rigshospitalet, Copenhagen University Hospital, Inge Lehmanns Vej 7, 2100 Copenhagen Ø, Denmark

[2] Faculty of Health and Medical Sciences, University of Copenhagen, Blegdamsvej 3B, 2200 Copenhagen N,, Denmark

[3] Copenhagen Academy for Medical Education and Simulation, Rigshospitalet, Copenhagen University Hospital, Blegdamsvej 9, 2100 Copenhagen Ø, Denmark

Fluorescence angiography with ICG (FA-ICG) has predominantly been performed using visual assessment of the fluorescence angiography (V-ICG), where the surgeon subjectively evaluates the fluorescence signal. Numerous reviews and meta-analysis have evaluated V-ICG, concluding that V-ICG does seem to decrease the rate of AL in colorectal and esophageal resections. However, the results could be considered biased, as the studies were heterogeneous, and no randomized studies were included [17, 19–22]. Recently, a meta-analysis that also included data from two new randomized trials found an odds ratio of 0.34, (95% CI 0.22–0.53; $p < 0.001$) for AL-following colorectal resections. While promising, the authors stated that the results were biased, as the included studies were heterogeneous and predominantly had a retrospective design [23]. These limitations of the studies mentioned above may be attributed to the subjective nature of V-ICG, emphasizing the need for objective FA-ICG assessment [19–23].

Quantifying the FA-ICG generates objective perfusion values, thus eliminating the subjective limitations of V-ICG, and several quantification methods have been presented [18, 24–26]. Here, instead of the surgeon visually assessing the FA-ICG, the fluorescent signal is processed by computer software generating a fluorescence-time-curve (FTC) [18] (Fig. 1). From this FTC, a range of different of Q-ICG parameters can be calculated, reflecting tissue perfusion [18]. Several Q-ICG parameters have been evaluated and have shown exciting results in the fields of plastic surgery [27, 28], ophthalmic surgery [29], and neurosurgery [30, 31]. These results conclude that Q-ICG is an accurate, objective, and unbiased method of perfusion assessment. However, Q-ICG is still a novel technology, and currently, no Q-ICG parameter or methodology is considered a gold standard.

This narrative review aims to provide a description of the state of intraoperative Q-ICG during gastrointestinal surgery and discuss its potential pitfalls when performed it in a clinical setting.

Intraoperative Q-ICG

Basic setup

Intraoperative Q-ICG requires four vital pieces of equipment: the fluorescent dye (indocyanine green), a near-infrared (NIR) camera, a recording system, and software for processing the recorded fluorescence signal. All systems that support FA can be utilized for intraoperative Q-ICG, considering they provide video output. Many different Q-ICG software systems are available, and a few commercial FA systems already offer build-in support for intraoperative Q-ICG [32–34]. Also, several custom software solutions have been developed, offering a more comprehensive range of Q-ICG parameters not currently available on the commercial market [18, 25, 35].

Methodology

Intraoperative Q-ICG can be performed in several ways; however, the essential steps are illustrated in Fig. 1.

The FTC and defining Q-ICG parameters

Q-ICG is based on the FTC (Figs. 2 and 3). The FTC is generated by a Q-ICG software system based on the average pixel intensity of a selected "region of interest" (ROI) and plotted against time. The FTC has different phases

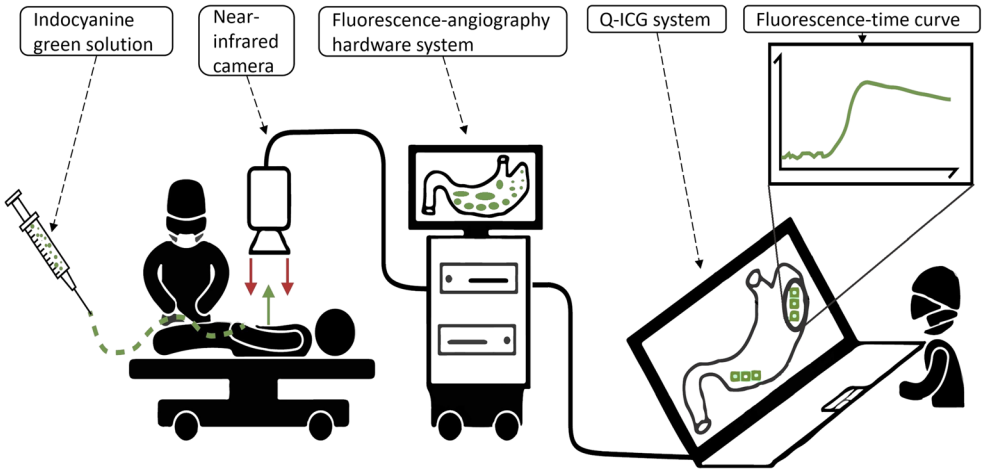

Fig. 1 Intraoperative Q-ICG setup and methodology. Phase 0: (**a**) The ICG solution and Q-ICG system are prepared. (**b**) The near-infrared camera is placed at a set angle and distance to the target tissue. (**c**) Regions of interest are placed in the Q-ICG system by the surgeon in white light. Phase 1: (**a**) The fluorescence angiography system is set to emit (red arrows) and detect near-infrared light (green arrows). (**b**) Immediately, ICG (0.25 mg/kg) is administered through a peripheral venous catheter followed by a saline flushing (10 mL). Phases 2 and 3: (**a**) The Q-ICG software system processes the fluorescence signal and generates a FTC. Subsequently, the system calculates Q-ICG parameters from the "regions of interest" selected by the surgeons

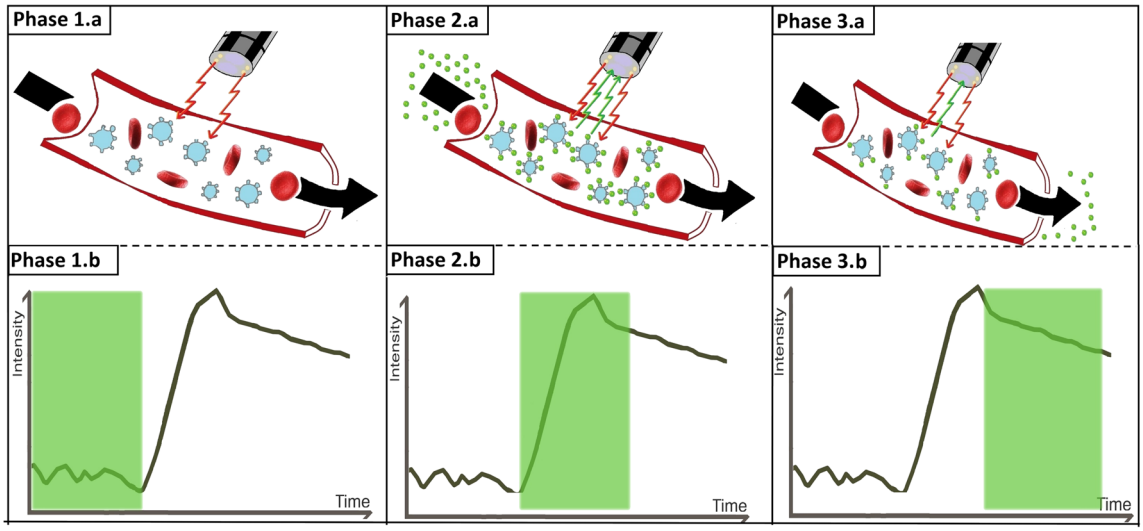

Fig. 2 A schematic overview of different Q-ICG phases. Phase 1: (**a**) The camera system is set to near-infrared mode, and ICG (0.25 mg/kg) is administered, followed by a saline flush. (**b**) The fluorescence-time-curve displays baseline static. Phase 2: (**a**) Plasma bound ICG begins to enter the target tissue. ICG molecules are excited by the near-infrared light and begin to fluoresce. (**b**) A steep increase in fluorescence intensity is observed. This is the inflow phase. Phase 3: (**a**) ICG is removed by hepatic clearance. Thus, less ICG is bound to plasma proteins. (**b**) fluorescence-time-curve displays a steady decline in fluorescence intensity. *Permission to re-use this illustration from the paper "*Laser speckle contrast imaging and quantitative fluorescence angiography for perfusion assessment*" was obtained from Springer Publishing

corresponding to the events that take place on a capillary level during the FA-ICG. An understanding of these events is necessary to select the optimal Q-ICG parameter, and the events can be divided into four phases (Figs. 1 and 2).

Phase 0—preparation The NIR camera equipment and ICG dye are prepared. The NIR-camera is fixed at a set distance and angulation to the area of interest (typically an area at risk for compromised perfusion). If immediate intraoperative Q-ICG analysis is desired, ROIs are placed by the surgeon in white light, and the recording is initiated.

Phase 1—ICG administration The camera system is turned from white light to NIR-mode, and ICG is subsequently

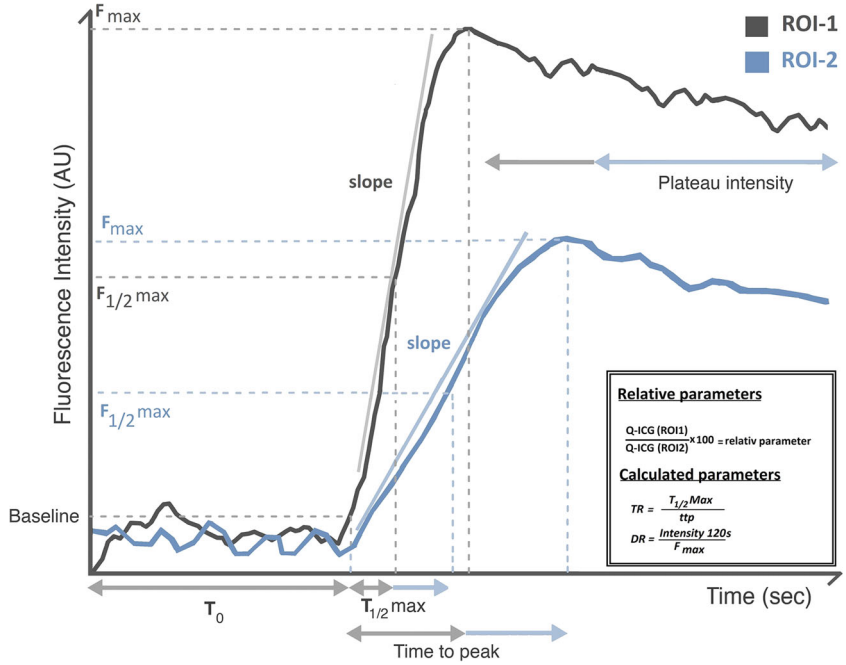

Fig. 3 Definition of Q-ICG parameters. A visual representation of the various Q-ICG parameters and relative parameters

administered intravenously, followed by a saline flush (5–10 mL). The delay from ICG administration to the first significant increase in fluorescence intensity is termed time to first fluorescence signal (*T*0). The FTC displays background static during this phase.

Phase 2—ICG inflow As ICG enters the target tissue, a steep increase in the fluorescence intensity of the FTC is observed (provided the tissue is perfused). The fluorescence intensity continues to increase until the maximum intensity (*F*max) is reached. This interval is termed time-to-peak (*ttp*) [25, 26, 36–39]. Three additional Q-ICG parameters can be derived from this part of the FTC; slope (*slp*), which is the differential to the FTC during the *ttp* interval; $T_{1/2\max}$ which is the time from the first intensity increase until 50% of maximum intensity is reached [25, 26, 37, 40] and the ratio between $T_{1/2}$max and *ttp* termed the time ratio (*TR*) [25].

Phase 3—ICG elimination As the ICG bolus passes the regions of interest and is eliminated from the vascular system, the FTC shows a corresponding decrease in intensity. Here an additional two Q-ICG parameters can be calculated; drainage ratio (*DR*), which is the absolute intensity value at 120 s divided by *F*max [41] and plateau intensity (*PI*), which is defined as the median value intensity in the last 25% of the FA-ICG [18].

A visual representation of the Q-ICG parameters (*F*max, *ttp*, *slp*, *PI*, *DR*, *TR*, and $T_{1/2\max}$) and the relative Q-ICG parameters can be seen in Fig. 3. For relative parameters, two ROIs are selected: One is the reference *ROI* (blue in Fig. 3) placed within an area with excellent perfusion, and the other is the target *ROI* (gray in Fig. 3) placed in an area at risk of reduced perfusion. The relative Q-ICG parameter is then obtained by dividing the target ROI with the reference ROI [42].

Intensity vs. inflow parameters

Q-ICG parameters can be divided into two categories: Intensity and inflow parameters. This separation is warranted as inflow parameters (*ttp*, *slp*, *norm slp*, $T_{1/2\max}$, and *T0*) are defined from the timing of distinct perfusion events, while intensity parameters (*F*max, *DR*, and *PI*) are based on absolute fluorescence measurements. Both categories of parameters have been examined in different settings: "perfusion correlation" comparing already established measures of microperfusion such as local lactate levels or radiolabeled microspheres with Q-ICG parameters and "exploratory endpoints" investigating the utility of Q-ICG parameters against set endpoints. However, these studies have prominently been in animal models.

Intensity parameters

Animal studies—perfusion correlation *F*max was correlated with radioactive microspheres perfusion in one study utilizing a normo-perfused porcine model. Here, it significantly correlated with the perfusion in two ROIs (Pearson's $r = 0.78$; $p = 0.04$ and $r = 0.88$; $p = 0.01$) [18]. *PI* had conflicting results when correlated with radioactive microspheres perfusion in a porcine model, rendering a significant correlation in one ROI ($r = 0.94$; $p < 0.01$) while the correlation was insignificant in another ($r = 0.64$; $p = 0.12$) [18].

Animal studies—exploratory endpoint In a study of 60 rats, the relative *F*max (R-*F*max) parameter was used to predict clinical necrosis on day three following bowel strangulation [41]. A receiver operating characteristic (ROC) analysis was performed, generating cutoff values and calculating the "area under the curve" (AUC). It was calculated that a perfusion level of 40% (AUC 0.75), determined by *R*-*F*max, corresponded to an OR of 5.0 ($p = 0.06$) for clinical necrosis. This performance was inferior when compared with standalone clinical assessment, with an OR of 19.2 ($p < 0.01$) for clinical necrosis.

Clinical studies—anastomotic leakage Several studies investigating patients undergoing colorectal or esophageal resection have analyzed if *F*max [25, 26, 36–38] or *R*-*F*max [39] could detect a difference in anastomotic perfusion between patients suffering from AL and patients without AL. Only a single study, utilizing *F*max, could present a significant difference between the two groups [26].

Inflow parameters

Animal studies—perfusion correlation studies The *slp* parameter was analyzed in four animal studies where it showed a linear correlation (Spearman's *rho*/Pearson's $r = 0.78$–0.97) with radioactive microspheres perfusion [18, 43, 44]. The *slp* parameter performed slightly better in a normo-perfused porcine model (Pearson's $r = 0.97$, $p = 0.001$) [18] compared with an arterial ischemia model in rabbits and porcine (*rho* = 0.78–0.90) [43, 44].

Two studies also utilized a normalized slope parameter to mathematical compensate for the fluctuations in fluorescence intensity caused by differences in the baseline and maximum intensity between test subjects [18, 45]. The normalized slope produced a strong correlation with local lactate levels in a normo-perfused porcine model (Pearson's $r = 0.96$, $p = 0.001$) [18] and an acceptable correlation with local lactate levels in an ischemic porcine model (*rho* = 0.77, $p < 0.001$) [45].

The *ttp* parameter has been analyzed in two porcine studies [18, 35] using either local lactate levels [35] or radioactive

microspheres as markers for perfusion [18]. Compared with radioactive microspheres in a normo-perfused model the *ttp* parameter rendered conflicting results, correlating in one ROI (Pearson's $r = -0.84$, $p = 0.02$), while not in another ROI (Pearson's $r = -0.67$, $p = 0.10$) [18]. When compared with local lactate levels in the ischemic ROIs, the *ttp* parameter performed well (*rho* = 0.71); however, its performance again decreased within a normo-perfused ROI (*rho* = 0.30) [35]. To our knowledge, no studies have investigated the validity of T0 or $T_{1/2max}$.

Animal studies—exploratory endpoint studies The relative time-to-peak (*R-ttp*) parameter was explored in a series of porcine studies to determine if intraoperative Q-ICG could help surgeons locate optimal sites for anastomosis [24, 42, 46].

The Q-ICG system was set to select clinically viable margins at a 50% increased *ttp* (e.g., reduced perfusion) compared with a well-perfused reference ROI. The "presumed clinically viable" margins selected by the Q-ICG system had significantly lower levels of local lactates compared with the margins selected by an unassisted surgeon [24, 46]. In another study, the Q-ICG system was set to select resections sites at 25%, and 75% of maximum perfusion based on *R-slp*. Here, an indicator of local ischemia (lactate levels) was significantly higher at the 25% site compared with the 75% site (3.7 mmol/L vs. 2.9 mmol/L, $p < 0.01$) [42].

Several other inflow parameters have been explored following a range of interventions, illustrated by the following examples: (1) A relative-norm-slope parameter could detect a pharmaceutically induced relative increase in anastomotic perfusion following a blinded, randomized, placebo-controlled administration of glucagon-like peptide 2 (GLP-2) in pigs undergoing a small bowel resection ($p < 0.05$) [47]. (2) A relative-slope parameter was used to identify sites for anastomosis at 30%, 60%, and 100% of relative perfusion. The anastomosis created at 30% relative perfusion had a significantly lower tensile strength than anastomoses created at 60% or 100% perfusion (9.09 N vs. 11.5 N and 12.9 N, $p < 0.05$) [48]. **3)** The relative-slope parameter could detect a significant reduction in intestinal perfusion of a rat bowel following intestinal manipulation. Compared with a reference ROI, the regional perfusion dropped from 100 to 61% ($p < 0.05$) directly following intestinal perfusion, and it further decreased to 41% ($p < 0.05$) at 24 h post manipulation [49].

Clinical studies—anastomotic leakage Clinical studies within the fields of esophageal and colorectal surgery have analyzed if the inflow parameters (*ttp*, *slp*, *T0*, or $T_{1/2max}$) could detect differences in perfusion between patients with and without AL [25, 26, 36–38, 40]. The results were conflicting; a majority of studies using *slp*, *T0*, or $T_{1/2max}$ did find a significant difference in perfusion between patients with and without AL [25, 26, 36, 38, 40]; however, each parameter has also failed to separate the groups in select studies.

In the case of *ttp*, three studies did find a significantly longer *ttp* interval in patients with AL compared with patients without AL [25, 26, 36]. However, *ttp* also failed to show a significant difference in three studies [37–39]. The *slp* parameter was only analyzed in three studies, and while it did show a significant difference in perfusion between patients with and without AL in some studies [25, 26], it also failed in one study [37]. The $T_{1/2max}$ parameter managed to identify a significant difference between patients with and without AL in three studies, and only failed in a single study [37]. Finally, the *T0* parameter showed a significantly longer *T*0 interval in patients with AL compared with patients without AL [37, 38], while one paper found no difference [26].

An important note is that none of the clinical studies performed intraoperative Q-ICG; instead, the Q-ICG analysis was performed post-hoc by analyzing video recordings of the FA. Consequently, these studies can mainly be utilized to identify high-performance parameters and establish cutoff values by ROC analysis. In a ROC analysis of colorectal anastomotic complications the following cutoff values were found $slp < 0.7$ AU/s (AUC = 0.12, $p = 0.002$), $T_{1/2max} > 18$ s (AUC = 0.96, $p < 0.001$) and $TR > 0.6$ (AUC = 0.93, $p < 0.001$) [25]. Another study looked at venous anastomotic failure and established a cutoff value of $T_{1/2max} > 9.6$ s (AUC = 0.82) [40]. These results, while illustrative, should be interpreted with caution as the studies were heterogeneous in design, mostly retrospective, and lacked matched or randomized control groups.

Challenges with intraoperative Q-ICG

The previous section illustrates that various Q-ICG parameters are validated for assessing visceral tissue perfusion and can detect changes in perfusion following a range of interventions. However, when interpreting the results of Q-ICG, one should be mindful that several factors may distort the validity of the Q-ICG readings:

Securing a fixed camera distance and set angulation toward the target tissue is critical as the fluorescence intensity decreases with increased camera distance due to the inverse-square law [50]. A similar argument applies to the angulation of the camera as with increased angulation to target ROI; less light illuminates the tissue and the lens [51]. Finally, a steady camera is optimal for reducing the number of movement artifacts. We recommend utilizing a mechanical holding arm or the "lock camera" feature on robotic equipment at a fixed distance with the steepest possible angulation to the target ROI.

1. The ICG-plasma concentration is critical, especially for Q-ICG parameters based on absolute values, as the

fluorescence intensity depends on the underlying ICG plasma concentration, c.f. Lambert-Beers Law [52]. Ensuring a stable and comparable ICG plasma concentration between patients is challenging as it depends on the distribution volume, regional perfusion, and rate of metabolism. Hence, a body mass-adjusted ICG administration (0.25 mg/kg) is preferable.

2. Systemic perfusion factors are likely to affect local fluorescence intensity, as local blood flow is depending on systemic parameters and influenced by cardiac output, blood pressure, and vasoconstriction [53]. We recommend continuous monitoring of these systemic perfusion factors during surgery, and that they should be considered when interpreting the Q-ICG results.
3. The diffusion/retrograde flow problem can distort the fluorescence intensity in select cases with compromised tissue perfusion. Initially, the FTC displays a low-intensity value and thus correctly reflects the compromised perfusion. However, the ICG concentration within the target ROI with reduced perfusion may increase due to overtime diffusion and retrograde flow, resulting in falsely inflated *F*max values [25, 42, 46]. As such, we recommend only using inflow parameters as this problem only affects intensity parameters.
4. Selection of representable ROIs. This factor depends on the surgeon's selection of representable ROIs while accounting for movement due to respiration or peristalsis during the FA. Furthermore, light reflections at the serosa side of the intestine can result in suboptimal ROI placement. Also, movement of the target ROI due to breathing or peristalsis is problematic and challenging to eliminate; however, one study has shown that a computerized motion-tracking can compensate for most of the movement [54].
5. Differences between FA systems. Various FA systems have different sources of excitatory light (LED vs. Halogen vs. Diode lasers) [17] and sensitivity to the fluorescence light (difference in filters and sensors). The measurement of the fluorescence intensity likely differs between two FA systems, even if all other factors are kept constant.

Recommendations for utilizing Q-ICG

We can conclude that the available studies on Q-ICG are heterogeneous both in terms of the investigated parameter, methodology, endpoints, and results. Hence, illustrating the apparent need for a consensus regarding the employment of Q-ICG in clinical practice. Also, the technology for intraoperative Q-ICG is currently available, but studies are investigating the performance of intraoperative Q-ICG are lacking. We, therefore, present the following suggestions regarding the three challenges that Q-ICG must overcome before it can become a practical tool in the clinic.

Selection of Q-ICG parameter Various Q-ICG parameters (*F*max, *ttp*, *slp*, and norm slp) have been validated in animal studies. However, some parameters (*F*max, *ttp*) performed inconsistently in clinical settings. The limited clinical performance of the *F*max parameter can likely be explained by its sensitivity to changes in camera distance and angulation, ROI selection, ICG plasma concentration, systemic perfusion factors, and the retrograde flow/diffusion problem. Thus, even if two hypothetical patients had the same perfusion, different *F*max values could still be rendered, as keeping all these factors constant between patients is extremely difficult in a clinical setting. The *ttp* parameter had superior performance to that of *F*max; however, still not satisfactory. The lack of performance cannot alone be explained by the Q-ICG challenges, as *ttp* is resilient to changes in camera distance, angulation, ICG plasma concentration, and the retrograde flow/diffusion problem. *Ttp* is resilient because it is resultant from the timing of the perfusion events rather than the exact fluorescence intensity measurements. However, *ttp* tended toward a weak correlation with perfusion, especially in well-perfused tissue [18, 35]. Consequently, *ttp* might have had difficulties in a clinical setting, as most patients are expected to have adequate tissue perfusion.

Slp and $T_{1/2max}$ had the best clinical performance for identifying AL patients, only failing in a single study that selectively included patients at high-risk for AL [37]. Both parameters are calculated from the inflow phase of the FTC. Experimental studies of perfusion in computer models have shown that the inflow phase of the FTC most accurately reflects the microperfusion [55, 56]. These findings are in accordance with the animal validations studies that found excellent correlations coefficients for *slp* and norm *slp* [18]. While no validation studies utilized $T_{1/2max}$, it does resemble *slp* from a mathematical point of view as it integrates both intensity and timing information during the critical inflow phase (Fig. 3). Furthermore, by utilizing *normalization*, one can modify the *slp* parameter to be based on relative changes in fluorescence intensity in a similar fashion to $T_{1/2max}$. Thereby significantly reducing the impact of several Q-ICG challenges that affect the measurement of the fluorescence intensity such as camera distance, angulation, ICG plasma concentration, and differences in FA camera systems [18, 45, 51].

Finally, the *T0* parameter, while not validated in any animal studies, did show a satisfactory clinical performance [37, 38]. It is based on the timing of fluorescence events in a similar fashion to *ttp* and, therefore, resilient to most of the Q-ICG challenges. *T0* is also easy and fast to use, and some studies have even examined it without using a computer. Instead, it was determined by the surgeons' assessment of the visual FA-

ICG [57–59]. However, *T0* suffers from a few unique problems as it may be influenced by peripheral vs. central venous catheter, catheter diameter, infusion speed, the height of the person, and vascular status [60]. In conclusion, we ultimately recommend using either the $T_{1/2max}$ or the *slp* parameter. An overview of the viability of the different parameters is presented in Table 1.

Options for intraoperative Q-ICG systems The current options for intraoperative Q-ICG are viable, as illustrated by one feasibility study that has developed a custom Q-ICG system. It reported an excellent system usability (SUS® of 82.5). Also, surgeons assisted by Q-ICG suggested sites for anastomosis with significantly higher perfusion than both surgeons in white light or with V-ICG [61]. Complementing the custom solutions are the commercial FA equipments that have begun to offers options for intraoperative Q-ICG [32–34]; however, most commercial systems only utilize the limited *F*max or *R-F*max parameters. Thus, future systems should be improved, drawing inspiration from studies that have already demonstrated intraoperative Q-ICG in both animals [24, 35, 42, 46] and patients [61, 62].

Interpreting the Q-ICG measurements An objective reference frame for Q-ICG parameters must be created as clinical decisions will remain subjective unless cutoff values are established. Hence, the next step for Q-ICG must be to develop procedure-specific cutoff values for the most common gastrointestinal procedures and clinical outcomes (anastomotic leakage, intestinal viability, etc.). Currently, only a few studies have established cutoff values for anastomotic and venous anastomotic failure based on *slp*, $T_{1/2max}$, *F*max, and *ttp* [25, 26, 40]. However, these cutoff values are still heterogeneous and not validated. Therefore, before establishing procedure-specific Q-ICG cutoff values, a few notes should be considered. The reproducibility and feasibility of the Q-ICG evaluations could be improved by utilizing relative Q-ICG parameters. This is because cutoff values based on relative parameters create an index of perfusion rather than being based on an exact numerical value. In a clinical setting, it is more feasible for a surgeon to interpret a relative perfusion index of 50% based on $T_{1/2max}$ rather than aim for a $T_{1/2max}$ value < 15 s (values are arbitrarily selected). Besides, relative parameters are less susceptible to the challenge that different FA systems poses. Despite these advantages, relative parameters have remained mostly unexplored in clinical settings.

Conclusion

Many Q-ICG parameters have been validated for perfusion assessment. However, Q-ICG parameters based on either intensity parameter (*R-F*max, *R-DR*, and *F*max) or timing parameters alone (*ttp*) have difficulties reflecting clinical endpoints. Instead, parameters that combine both timing and intensity during the inflow phase ($T_{1/2max}$ and *slp*) does reflect clinical endpoints. These parameters are also less sensitive to most of the factors that challenge intraoperative Q-ICG. Thus, we recommend using the methodology outlined in this review with a mass-depended ICG dosing (0.25 mg/kg), fixated NIR camera setup, stable systemic perfusion factors, and utilizing either the $T_{1/2max}$ or *slp* parameter. Furthermore, while intraoperative Q-ICG predominantly has been performed in animal studies, recent clinical studies have proven that intraoperative Q-ICG is technically feasible with both commercial and custom software solutions. Thus, the next step for Q-ICG will be

Table 1 A semi-quantitative assessment of Q-ICG parameters

	Performance in animal perfusion correlation studies	Clinical performance	Resilience to Q-ICG challenges
Intensity parameter			
*F*max	★★☆	☆☆☆	☆☆☆
PI	★☆☆	N.A	☆☆☆
DR	N.A	N.A	☆☆☆
Inflow parameter			
Slp	★★★	★★☆	★★☆
Norm *slp*	★★★	N.A	★★★
$T_{1/2}$max	N.A	★★★	★★★
ttp	★★☆	★★☆	★★★
T0	N.A	★★☆	★★★
TR	N.A	★★☆	★★☆

Fmax, maximum fluorescence intensity; *PI*, plateau intensity; *DR*, drainage ratio; *slp*, slope; norm *slp*, normalized slope; $T_{1/2max}$, time to 50% of maximum intensity; *ttp*, time-to-peak; *T0*, time to first fluorescence signal; *TR*, time ratio; *N.A*, not applicable

to establish procedure-specific cutoff values that will allow surgeons to make decisions based on objective and unbiased perfusion assessments.

Limitations

This narrative review is based on expert knowledge of the topic rather than a systematic literature review. As such, we cannot exclude that relevant studies have been overlooked. Also, arguments and views presented in this review are based on the author's knowledge of Q-ICG; however, support from the literature has been sought when possible. Q-ICG is still a novel tool, and the heterogeneity between published studies limits the possibilities for a meta-analysis.

Compliance with Ethical Standards

Conflict of interest The authors declare that they have no conflicts of interest.

Research involving human participants and animals This narrative review is based on already published peer-reviewed articles. All included animal studies reported to follow the institutional guidelines for animal experiments. All included human studies reported to follow local institutional guidelines for human trials.

Informed consent All studies performed by other authors that included human participants had obtained informed written consent.

References

1. Matienzo D, Bordoni B (2020) Anatomy, blood flow, in StatPearls. StatPearls Publishing. Copyright © 2020, StatPearls Publishing LLC., Treasure Island (FL).
2. Robson MC, Steed DL, Franz MG (2001) Wound healing: biologic features and approaches to maximize healing trajectories. Curr Probl Surg 38(2):72–140
3. Shandall A, Lowndes R, Young HL (1985) Colonic anastomotic healing and oxygen tension. Br J Surg 72(8):606–609
4. Thompson SK, Chang EY, Jobe BA (2006) Clinical review: healing in gastrointestinal anastomoses, part I. Microsurgery 26(3):131–136
5. Kassis ES et al (2013) Predictors of anastomotic leak after esophagectomy: an analysis of the society of thoracic surgeons general thoracic database. Ann Thorac Surg 96(6):1919–1926
6. Pommergaard HC et al (2015) Impaired blood supply in the colonic anastomosis in mice compromises healing. Int Surg 100(1):70–76
7. Vignali A et al (2000) Altered microperfusion at the rectal stump is predictive for rectal anastomotic leak. Dis Colon Rectum 43(1):76–82
8. Burton TP, Mittal A, Soop M (2013) Nonsteroidal anti-inflammatory drugs and anastomotic dehiscence in bowel surgery: systematic review and meta-analysis of randomized, controlled trials. Dis Colon Rectum 56(1):126–134
9. Chioreso C et al (2018) Association between hospital and surgeon volume and rectal cancer surgery outcomes in patients with rectal cancer treated since 2000: systematic literature review and meta-analysis. Dis Colon Rectum 61(11):1320–1332
10. Gershuni VM, Friedman ES (2019) The microbiome-host interaction as a potential driver of anastomotic leak. Curr Gastroenterol Rep 21(1):4
11. Trencheva K et al (2013) Identifying important predictors for anastomotic leak after colon and rectal resection: prospective study on 616 patients. Ann Surg 257(1):108–113
12. Urbanavicius L et al (2011) How to assess intestinal viability during surgery: a review of techniques. World J Gastrointest Surg 3(5):59–69
13. Karliczek A et al (2009) Surgeons lack predictive accuracy for anastomotic leakage in gastrointestinal surgery. Int J Color Dis 24(5):569–576
14. Huang L, Li TJ (2018) Laparoscopic surgery for gastric cancer: where are we now and where are we going? Expert Rev Anticancer Ther 18(11):1145–1157
15. Nakauchi M et al (2017) Robotic surgery for the upper gastrointestinal tract: current status and future perspectives. Asian J Endosc Surg 10(4):354–363
16. Garski TR et al (1978) Adverse reactions after administration of indocyanine green. Jama 240(7):635
17. Alander JT et al (2012) A review of indocyanine green fluorescent imaging in surgery. Int J Biomed Imaging 2012:940585
18. Nerup N et al (2017) Quantification of fluorescence angiography in a porcine model. Langenbeck's Arch Surg 402(4):655–662
19. Degett TH, Andersen HS, Gogenur I (2016) Indocyanine green fluorescence angiography for intraoperative assessment of gastrointestinal anastomotic perfusion: a systematic review of clinical trials. Langenbeck's Arch Surg 401(6):767–775
20. Jansen SM et al (2018) Optical techniques for perfusion monitoring of the gastric tube after esophagectomy: a review of technologies and thresholds. Dis Esophagus 1:31(6)
21. Ladak F et al (2019) Indocyanine green for the prevention of anastomotic leaks following esophagectomy: a meta-analysis. Surg Endo 33(2):384–394.
22. Slooter MD et al (2019) Fluorescent imaging using indocyanine green during esophagectomy to prevent surgical morbidity: a systematic review and meta-analysis. J Thorac Dis: S755–S765
23. Arezzo A et al (2020) Intraoperative use of fluorescence with indocyanine green reduces anastomotic leak rates in rectal cancer surgery: an individual participant data analysis. Surg Endosc (Online ahead of print)
24. Diana M et al (2014) Real-time navigation by fluorescence-based enhanced reality for precise estimation of future anastomotic site in digestive surgery. Surg Endosc 28(11):3108–3118
25. Son GM et al (2019) Quantitative analysis of colon perfusion pattern using indocyanine green (ICG) angiography in laparoscopic colorectal surgery. Surg Endosc 33(5):1640–1649
26. Wada T et al (2017) ICG fluorescence imaging for quantitative evaluation of colonic perfusion in laparoscopic colorectal surgery. Surg Endosc 31(10):4184–4193
27. Li K et al (2018) Application of indocyanine green in flap surgery: a systematic review. J Reconstr Microsurg 34(2):77–86
28. Pruimboom T et al (2019) Optimizing indocyanine green fluorescence angiography in reconstructive flap surgery: a systematic review and ex vivo experiments. Surg Innov: (1):103–11
29. Herbort CP Jr et al (2017) Failure to integrate quantitative measurement methods of ocular inflammation hampers clinical practice and trials on new therapies for posterior uveitis. J Ocul Pharmacol Ther 33(4):263–277
30. Simal-Julián JA et al (2015) Indocyanine green videoangiography methodological variations: review. Neurosurg Rev 38(1):49–57 discussion 57
31. Cavallo C et al (2019) Applications of microscope-integrated indocyanine green videoangiography in cerebral revascularization procedures. Front Surg 6:59

32. Bigdeli AK et al (2016) Indocyanine green fluorescence for free-flap perfusion imaging revisited: advanced decision making by virtual perfusion reality in visionsense fusion imaging angiography. Surg Innov 23(3):249–260
33. Sood M, Glat P (2013) Potential of the SPY intraoperative perfusion assessment system to reduce ischemic complications in immediate postmastectomy breast reconstruction. Ann Surg Innov Res 7(1):9–9
34. Ye X et al (2013) Clinical values of intraoperative indocyanine green fluorescence video angiography with Flow 800 software in cerebrovascular surgery. Chin Med J 126(22):4232–4237
35. Diana M et al (2014) Enhanced-reality video fluorescence: a real-time assessment of intestinal viability. Ann Surg 259(4):700–707
36. Amagai H et al (2019) Clinical utility of transanal indocyanine green near-infrared fluorescence imaging for evaluation of colorectal anastomotic perfusion. Surg Endosc (Online ahead of print). https://doi.org/10.1007/s00464-019-07315-7
37. Hayami S et al (2019) Visualization and quantification of anastomotic perfusion in colorectal surgery using near-infrared fluorescence. Tech Coloproctol 23(10):973–980
38. Iwamoto H et al (2020) Quantitative indocyanine green fluorescence imaging used to predict anastomotic leakage focused on rectal stump during laparoscopic anterior resection. J Laparoendosc Adv Surg Tech A 30(5):542–546
39. Kim JC, Lee JL, Park SH (2017) Interpretative guidelines and possible indications for indocyanine green fluorescence imaging in robot-assisted sphincter-saving operations. Dis Colon Rectum 60(4):376–384
40. Kamiya K et al (2015) Quantitative assessment of the free jejunal graft perfusion. J Surg Res 194(2):394–399
41. Matsui A et al (2011) Predicting the survival of experimental ischemic small bowel using intraoperative near-infrared fluorescence angiography. Br J Surg 98:1725–1734
42. Diana M et al (2015) Intraoperative fluorescence-based enhanced reality laparoscopic real-time imaging to assess bowel perfusion at the anastomotic site in an experimental model. Br J Surg 102(2): e169–e176
43. Toens C et al (2006) Validation of IC-VIEW fluorescence videography in a rabbit model of mesenteric ischaemia and reperfusion. Int J Color Dis 21(4):332–338
44. Quero G et al (2019) Discrimination between arterial and venous bowel ischemia by computer-assisted analysis of the fluorescent signal. Surg Endosc 33(6):1988–1997
45. Ronn JH et al (2019) Laser speckle contrast imaging and quantitative fluorescence angiography for perfusion assessment. Langenbeck's Arch Surg 404(4):505–515
46. Diana M et al (2014) Probe-based confocal laser endomicroscopy and fluorescence-based enhanced reality for real-time assessment of intestinal microcirculation in a porcine model of sigmoid ischemia. Surg Endosc 28(11):3224–3233
47. Nerup N et al (2018) Quantitative perfusion assessment of intestinal anastomoses in pigs treated with glucagon-like peptide 2. Langenbeck's Arch Surg 403(7):881–889
48. Gosvig K et al (2019) Remote computer-assisted analysis of ICG fluorescence signal for evaluation of small intestinal anastomotic perfusion: a blinded, randomized, experimental trial. Surg Endosc 34(5):2095–2102
49. Behrendt FF et al (2004) Indocyanine green fluorescence measurement of intestinal transit and gut perfusion after intestinal manipulation. Eur Surg Res 36(4):210–218
50. Brownson JRS (2014) Solar energy conversion systems. Vol. Chapter 3. Academic Press, p41–66
51. Nerup N et al (2017) Reproducibility and reliability of repeated quantitative fluorescence angiography. Surg Technol Int 31:35–39
52. Swinehart DF (1962) The Beer-Lambert law. J Chem Educ 39(7): 333
53. Desmettre T, Devoisselle JM, Mordon S (2000) Fluorescence properties and metabolic features of indocyanine green (ICG) as related to angiography. Surv Ophthalmol 45(1):15–27
54. Selka F et al (2014) Fluorescence-based enhanced reality for colorectal endoscopic surgery. In: Biomedical Image Registration. Springer International Publishing, Cham
55. Choi M et al (2011) Dynamic fluorescence imaging for multiparametric measurement of tumor vasculature. J Biomed Opt 16(4):046008
56. Prasetya H et al (2019) Estimation of microvascular perfusion after esophagectomy: a quantitative model of dynamic fluorescence imaging. Med Biol Eng Comput 57(9):1889–1900
57. Kumagai Y et al (2018) Indocyanine green fluorescence angiography of the reconstructed gastric tube during esophagectomy: efficacy of the 90-second rule. Dis Esophagus 31(12):1
58. Kumagai Y et al (2014) Hemodynamics of the reconstructed gastric tube during esophagectomy: assessment of outcomes with indocyanine green fluorescence. World J Surg 38(1):138–143
59. Ohi M et al (2017) Prevalence of anastomotic leak and the impact of indocyanine green fluorescein imaging for evaluating blood flow in the gastric conduit following esophageal cancer surgery. Esophagus 14(4):351–359
60. Kim T et al (1998) Effects of injection rates of contrast material on arterial phase hepatic CT. AJR Am J Roentgenol 171(2):429–432
61. Nerup N et al (2020) Feasibility and usability of real-time intraoperative quantitative fluorescent-guided perfusion assessment during resection of gastroesophageal junction cancer. Langenbeck's Arch Surg 405(2):215-222
62. Green JM 3rd et al (2015) Intraoperative fluorescence angiography: a review of applications and outcomes in war-related trauma. Mil Med 180(3 Suppl):37–43

Publisher's note Springer Nature remains neutral with regard to jurisdictional claims in published maps and institutional affiliations.